MHD Steady Three-Dimensional Stagnation Point Flow of a Nanofluid Past a Circular Cylinder

A Thesis Submitted in Partial Fulfillment for the Requirement of the Degree of

Master of Philosophy in Mathematics By

Naeem Ullah

Supervised by

Prof. Dr. Sohail Nadeem

Department of Mathematics

Quaid-i-Azam University
Islamabad, Pakistan

2017

Dedicated to

My parents.

Preface

Magneto-hydrodynamic (MHD) is involved with the mutual interaction of magnetic field and fluid flow. There are significant applications of MHD ranges from astrophysics to modern technologies. MHD is typically used in industry to heat, pump, stir and levitate liquid metals. In the earth core, the fluid motion maintains the terrestrial magnetic field, the sunspots, and solar flares are generated by solar magnetic field and the galactic magnetic field which has the connections with star formation from the interstellar clouds. The static magnetic field is applied for the laminarization of contactless damping turbulent flow in the formation of semiconductor crystals or the continuous casting of steel. MHD flow concerns the behavior of particles in turbulent MHD flows which has been discussed by Rouson et al. [1]. In many natural phenomena, MHD effects occur such as, in the generation of a magnetic field of stars and planets. The interaction of earth magnetic field with the solar wind, generate northern lights, in which the magnetic field deflect the harmful cosmic rays. Hartlep and Mansour [2] discussed the utilization of MHD waves into a code for the replication of solar interior. Ripoll and Colestock [3] worked out on the development of a code for the modeling of lightning strikes.

Nanofluids are the colloidal suspensions of nanomaterials which is prepared by dispersing nanometer-sized materials, i.e. nanoparticles, nanofibers, nanotubes, nanowires and nanorods along with the base fluids. Water, oil, and ethylene glycol are Commonly used base fluids. Choi et al. [4] introduce the concept of nanofluids in order to generate fluids that have higher conductivities and rate of heat transfer. Nanofluids have fictional characteristics which make them potentially useful, due to its wide range of applications nanofluids got more attention. It is used as a cooling agent in electronic equipment, vehicles, heavy-duty engine and in industries to enhance the efficiency, saving energy and reduce emissions. Nanofluids have also some biomedical applications, it is used as an antibacterial and in drug delivery. Some admissible investigations by the researcher about nanofluids can be noticed in [5–10].

Stagnation point is the region where the of velocity of fluid becomes zero, or we can say that the flow around a body always has stagnation point. In boundary layer flow the stagnation flow profile has distinct and unique applications. It is used as a cooling agent in electronic devices, nuclear reactor, and other hydrodynamic activities. For an incompressible flow, researcher worked out the stagnation flow in three dimensions, oblique and orthogonal. Hiemenz [11] Investigated two-dimensional flow of a viscous fluid under stagnation point. In oblique stagnation flow, a rapid stream of fluid impinges in an oblique way on the solid wall at some angle. Stuart [12] initiated the flow of Newtonian fluid nearby the stagnation point. Homman [13] and Howarth [14] prescribed the steady flow of viscous fluid in three dimensions along the stagnation point. Due to its novel properties in industries nanofluids got the attention of researcher and they work on the stagnation flow of nanofluids. Hamad and Ferdows [15] analyzed the heat generation in nanofluid flow in the presence of stagnation point, they use the lie symmetries for the formulation of the problem. Nadeem et al. [16] inspected the flow of nano second-grade fluid near the stagnation point and got results via homotopy analysis method for different parameters. Nadeem et al. [17] explored the axisymmetric flow of micropolar nanofluid at stagnation point over a moving cylinder.

MHD stagnation point flow has been scrutinized by many researchers in the recent years. Bhattacharyya and Gupta [18] examined the heat transfer and flow along stagnation point on a porous surface in three-dimensions subject to a uniform magnetic field. Gireesha et al. [19] recognized the characteristics of an electrified fluid at stagnation-point with heat absorption or generation, melting and induced magnetic field effect past a stretching surface. Nadeem et al. [20] exposed the flow of Casson fluid in two-dimensions obliquely with the influence of the magnetic field and partial slip. Noor et al. [21] reviewed the flow of micropolar nanofluid along stagnation point by a stretched surface combined with heat transfer effects. Akbar et al. [22] observed nanofluid flow at the point of stagnation with the impact of magnetohydrodynamics aver a stretched cylinder and evaluated the flow problem numerically. Haq et al. [23] considered the effect of thermal radiation and magnetohydrodynamic flow of nanofluid over a stretchable sheet at the stagnation point. Makinde et al. [24] checked the flow of nanofluid at stagnation point passed over an elastic surface, and utilized the effect of magnetic field, convective heat, and buoyancy force. Ibrahim et al. [25] reported an article about the flow of nanofluid at stagnation point over an expandable sheet an account with heat transfer and magnetic field effect. Mansur et al. [26] exhibited the magnetohydrodynamic flow along stagnation point over a shrinking surface with suction. Hayat et al. [27] searched out the magnetohydrodynamic nanofluid flow in three dimensions along with the impact of thermal radiation. Zhang et al. [28] explained the MHD flow of nanofluid and describe the effect of radiation heat transfer and chemical reactions. Dinarvand et al. [29] sought out the unsteady flow of viscous fluid caused by a rotating sphere near the stagnation point in the presence of buoyancy forces. Howarth [30] described the flow behavior of steady incompressible fluid near the nodal stagnation point. Davey [31] identified the flow in the vicinity of the saddle point.

Declaration

With these words, I proclaim that this dissertation with title **"MHD steady three-dimensional stagnation point flow of a nanofluid past a circular cylinder**" is the research effort by me at Department of Mathematics, Quaid-I-Azam University, Islamabad, Pakistan. I finalize this report for the degree of Master of Philosophy in Mathematics under the kind supervision of **Prof. Dr. Sohail Nadeem**. The detail put forward is based on my own research work, and is not issued anywhere in the book or an article. The present thesis has not been complied anywhere for any other qualification or degree neither in this nor any other university.

Signature:______________________

Name:_________________________

Acknowledgement

First of all thanks to Almighty Allah S.W.T, all praises belonging to Allah S.W.T creator of all the words, the most benevolent, the most merciful, who strengthen me to accomplish this thesis.

I aspire to express my sincere recognition to my idol, and my supervisor **Prof. Dr. Sohail Nadeem** for his support, his generosity and kindness. His useful hints able me to complete my research work, I have a good and memorable experience to have with him, and will remember his good attitude, I am honored to have with him.

I wish to manifest my heartfelt appreciation to **Arif Ullah Khan**, my labfellow a PhD scholar in mathematics, for his support, fruitful discussions and providing necessary facilities. His expert guidance, precious suggestion and virtuous support enabled me to complete my research.

Also, special thanks to **Noor Muhammad**, my labmate a PhD scholar in mathematics for motivating me to carry on and was always interested in my personal development, and discussion with him is beneficial for me in this study. I would like to phrase my cordial acknowledge to my best friends **Latif Ahmed** a PhD scholar in mathematics, and **Abdur Rahman** Master of Philosophy in business administration, their encouragement, innovative consolation and help led me to finalize this work. They are keen in my personal improvement, their company is wonderful and memorable.

Finally I am grateful to my family, my parents, brothers and sister, their prayers and blessing enable me to complete my research work, my effort is all due to their unfailing support and encouragement throughout my studies, without them my work and studies would not have been possible. Thank you.

Naeem Ullah

2017

Contents

Chapter 1

Preliminary concepts

The incentive of this chapter is to manifest some basic definitions and pertinent properties of fluids, also some essential laws relevant to nanofluids are recalled.

1.1 Fluid

A material that deforms permanently and continuously under the action of shear stress (the ratio of tangential force to the area on which it is acted) no matter how small it is, or another word a substance in liquid and gas phase is referred to be a fluid.

1.2 Fluid mechanics

Fluid mechanics is the science that deals with the fundamental laws of general mechanics, which is applied to the fluids. These laws are conservation of momentum, conservation of energy and Newton's laws of motion, or we can say that fluid mechanics is a field of study, which characterizes the behavior of liquid and gases in motion or at rest. There are two main sub discipline of fluid mechanics.

1.2.1 Fluid dynamics

The subdivision of fluid mechanics that cover the behavior of fluid in motion, or that sort out the movement of fluids and the influence of forces on it.

1.2.2 Fluid statics

Fluid statics is the subdivision of fluid mechanics that investigate about the fluid in rest, i.e, when there is no shear stress and any other force developed is only due to the normal stress(pressure).

1.3 Flow

Movement of fluid under the action of unequal forces or stresses, as long as the unbalanced forces are applied the motion continues.

1.3.1 Laminar flow

The flow that occurs at lower velocities, in laminar flow the fluid particles move in a straight line not necessarily the velocity of particles at one point is the same as that of another line. The flow of high viscosity fluid is typically laminar.

1.3.2 Turbulent flow

The paths of fluid particles in a turbulent flow are no longer straight but are intertwining, sinuous and crossing one another. Velocity, pressure, and other flow quantities fluctuate in a disordered manner with time and space. The turbulent flow occurs mainly in low viscosity and high-velocity fluid.

1.4 Magneto-hydrodynamics

Magneto-hydrodynamics indicates the magnetic behavior of conducting fluid in the presence of an electric and magnetic field. Magneto-hydrodynamics affects many natural phenomena and also control turbulence within the flow.

1.5 Stagnation point

The point where the velocity of fluid becomes zero. Stagnation point occurs when a fluid strikes a non-rotating object, or in the movement of an obstacle through a fluid. At a stagnation point, the velocity components are zero, and their gradients are positive, also the pressure is the absolute maximum at that point.

1.6 Nanofluids

Nanofluids are the colloidal suspension of base fluids and nanoparticles. Nanoparticles are nanometer-sized particles or width of one-tenth thousand of a human hair. They are generally metal oxides or metals and usually, base fluids are taken water, ethylene glycol, and oil. Some unique features of nanofluids that make them potentially useful are as follow

* **Abnormal rise in thermal conductivity**

  The main feature of nanofluids is that, it has higher values of thermal conductivity.

* **Particle size dependence**

  It was observed that the decreasing particle size, there is an enhancement in thermal conductivity of nanofluids.

* **Stability**

  Nanofluid is used as a stabilizing agent.

* **Small concentration and a newtonian behavior**

For a very small concentration of nanoparticles, enough improvement in conductivity can be achieved, that shows completely Newtonian behavior.

1.6.1 Applications of nanofluids

Nanofluids have a wide range of applications, some specific areas where nanofluid can be used are

(a) Medical nanofluids(drug delivery and anti-bacterial agent).

(b) Bio and pharmaceutical nanofluids.

(c) Environmental nanofluids(pollution cleaner).

(d) Extraction nanofluids.

(e) Chemical nanofluids.

(f) Tribological nanofluids.

(g) Surfactant nanofluids.

Other applications of nanoparticles are listed in the figure below.

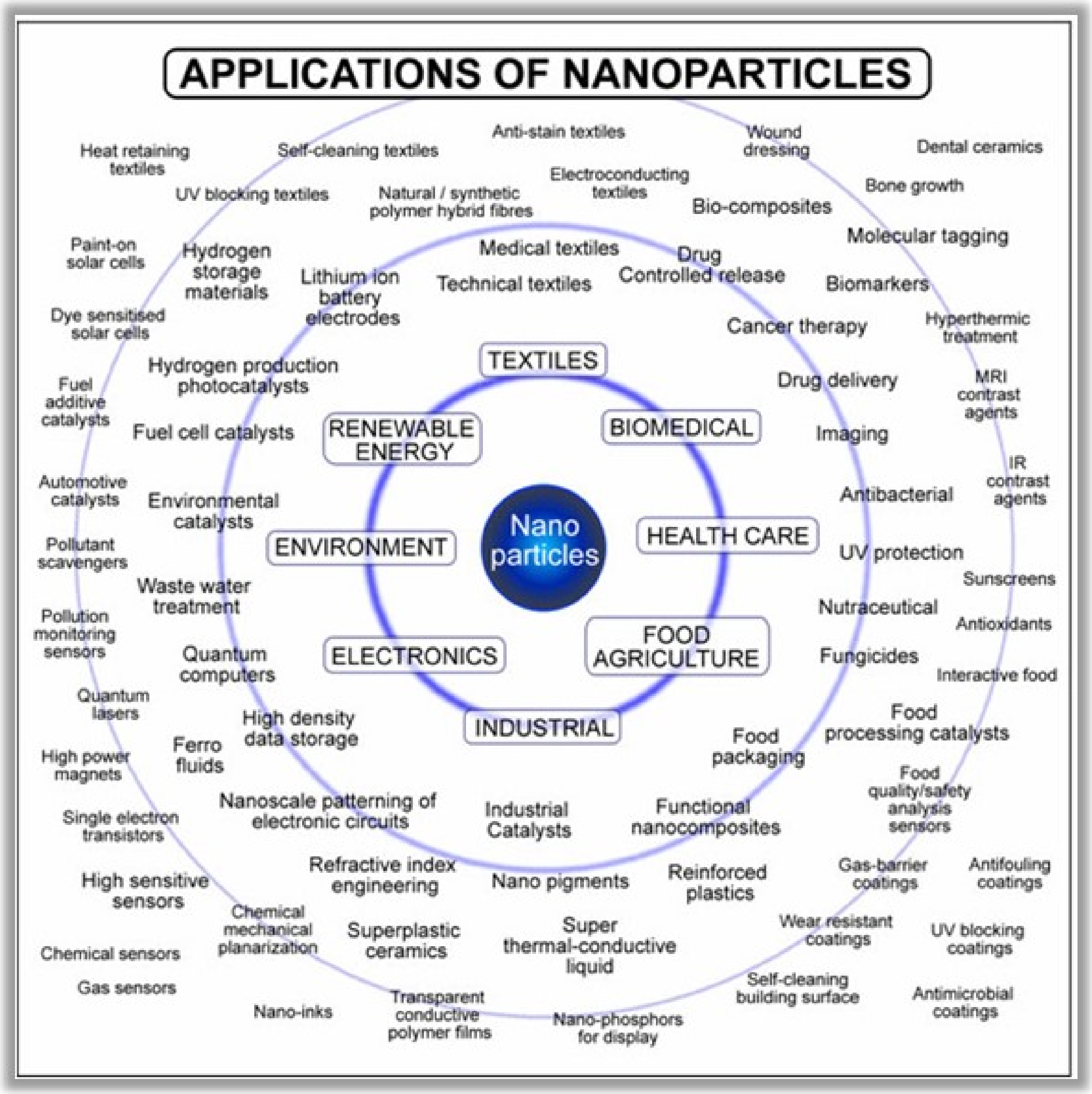

Figure 1.1: Applications of Nanomaterials Chart Picture

1.6.2 Physical properties of nanofluids

Thermal conductivity

Thermal conductivity is the heat conduction capacity of a substance, since metals are the good conductors of heat, using this feature, the nano-metallic particles are added to thermo-fluid in order enhance its thermal conductivity. Maxwell [32] formulated it as.

$$\frac{k_{nf}}{k_f} = \frac{k_p + 2k_f - 2\phi(k_f - k_p)}{k_p + 2k_f + \phi(k_f - k_p)} \tag{1.6.1}$$

Viscosity of nanofluids

Viscosity is the resistance of a fluid to flow, in the case of nanofluid, it is very important in its applications. Brinkman [33] model for the viscosity of nanofluid is given by

$$\mu_{nf} = \frac{\mu_f}{(1-\phi)^{2.5}} \tag{1.6.2}$$

Specific heat

Specific heat is the amount of heat per unit mass to raise the temperature up to a certain interval, so in the solid-liquid mixture this property is very important and is decreased by increasing particle volume fraction. According to Pak and Cho [34] representation of specific heat for nanofluid is shown as

$$(\rho C_p)_{nf} = (1-\phi)(\rho C_p)_f + \phi(\rho C_p)_p \tag{1.6.3}$$

Density of nanofluids

Xaun and Roetzel [35] Presented a model for nanofluid which is given by

$$\rho_{nf} = (1-\phi)\rho_f + \phi\rho_p \tag{1.6.4}$$

1.6.3 Equations for two phase model

Momentum equation

Generally, law of conservation of momentum for nanofluid can be written as

$$\rho_{nf}\frac{d\mathbf{V}}{dt} = div\boldsymbol{\tau} + \rho_{nf}\mathbf{b} \tag{1.6.5}$$

where $\mathbf{b}$ and τ are the body forces and the Cauchy stress tensor written as

$$\boldsymbol{\tau} = -p\mathbf{I} + \mu_{nf}\mathbf{A}_1 \tag{1.6.6}$$

in which $\mathbf{A}_1$ is first-order Rivlin-Ericksen tensor, expressed as

$$\mathbf{A}_1 = \nabla\mathbf{V} + (\nabla\mathbf{V})^t. \tag{1.6.7}$$

Energy equation

Generalized energy equation can be expressed as

$$(\rho C_p)_{nf}\frac{d\mathbf{T}}{dt} = \boldsymbol{\tau}.\mathbf{L} + k_{nf}\nabla^2\mathbf{T} - divq_r \tag{1.6.8}$$

where $\mathbf{L}$ is the gradient of velocity and q_r is radiative heat transfer.

1.7 Dimensionless quantities

1.7.1 Reynolds number

Reynolds number (R_e) was introduced by Stokes [36], it describes the flow behavior of the different fluids. It is the fraction of inertial force to the viscous force. It illustrates whether the flow is laminar or turbulent, so we have for smaller Reynolds number, there is a laminar flow while turbulent flow occurs at high Reynolds number.

$$R_e = \frac{\text{inertial force}}{\text{viscous force}} = \frac{ma}{\mu(u/x)x^2} = \frac{Ux}{\nu} \tag{1.7.1}$$

U is the maximum velocity of the object, measured in m/s, x identify the characteristic length traveled by fluid, its unit is m, ν denotes the kinematic viscosity, in SI its unit is m^2/s.

1.7.2 Prandtl number

Prandtl number determine the heat flux between a solid body and moving fluid. It specifies the ratio of momentum diffusivity to thermal diffusivity. It can be shown as

$$\begin{aligned} Pr &= \frac{\text{momentum diffusivity}}{\text{theremal diffusivity}} = \frac{\nu}{\alpha} \\ &= \frac{\mu C_p}{k} \end{aligned} \tag{1.7.2}$$

μ is the dynamic viscosity with unit Ns/m^2.

C_p shows the specific heat, in SI its unit is $j/kg - K$.

k is the thermal conductivity it is measured in $W/m - K$.

Prandtl number was introduced by a German physicist Ludwig Prandtl as reported by (Vogel-Prandtl [37]). Prandtl number has great importance in boundary-layer problems. Conduction occurs for a small value of Prandtl number, means that thermal boundary layer is thicker than velocity boundary layer. While for larger values, convection process occurs, which is more effective than conduction in transferring energy.

1.7.3 Magnetic-Prandtl number (M)

The magnetic Prandtl number predict the relative balance between momentum diffusivity and magnetic diffusivity written as

$$M = \frac{\nu}{\eta} = \sigma \mu_e \nu \tag{1.7.3}$$

σ is electrical conductivity of fluid its unit within the system international is S/m,
S is siemens, which is the inverse of ohm,
μ_e is the magnetic permeability, which tells about whether a material can be magnetized or not, its SI unit is N/A^2,
η is magnetic diffusivity, its unit is m^2/s.

1.7.4 Skin friction

The friction arises when the fluid moves through a solid surface or the friction due to the viscous resistance at the boundary in the flow. It affects the flow characteristics. The skin friction has larger value for laminar flow and has small values for turbulent flow, mathematically we can write as

$$C_f = \frac{\tau_w}{\rho_f U_w^2}. \tag{1.7.4}$$

In the above expression τ_w is the surface shear stress, ρ_f denotes the density of the fluid and U_w is the wall velocity.

1.7.5 Nusselt number

Nusselt number is the dimensionless quantity that associates heat transfer rate in the fluid, i.e. The convection to conduction heat transfer. Nusselt number can be express as

$$N_{u_x} = \frac{\text{coefficient of convection}}{\text{coefficient of conduction}} = \frac{h_x L}{k_f} \tag{1.7.5}$$

In convection heat transfer we have, $h_x = \frac{Q_w}{(T_s - T_\infty)}$, and by conduction, we have $Q_w = -k_f \nabla T$. Generally, we can write

$$N_{u_x} = \frac{h_x}{k_f} = C\ Re_x^m\ P_r^n. \tag{1.7.6}$$

Chapter 2

Steady three dimensional stagnation point flow of a nanofluid past a circular cylinder with sinusoidal radius variation

2.1 Introduction

In this chapter, we have studied the three-dimensional flow at the stagnation point of nanofluid over a cylinder with wavy radius. The governing boundary layer equations are non-dimensionalized using some specific transformations. The reduced problem to a system of coupled non-linear ordinary differential equations is then solved numerically using fifth order R-K-Fehlberg method. Nanofluids discussed here are copper, alumina, and titania taking water as a base fluid. The influence of nanoparticle volume fraction and distinct nanoparticles on velocities and temperature field are examined for both critical points. The dimensionless heat transfer rate and surface drag across the wall vary with the volume fraction of different nanoparticles, and their numerical results are listed in Table 2.2.

2.2 Flow structure

Here the fluid is passed over a cylinder in three dimensions considering y- and z-axis along and normal to the surface, and x-axis in the upward direction. Howarth [38] considered the velocity components near critical points as $u_e = ax$ and $v_e = by$, with a and b are constants. The surface is at temperature T_s and the fluid is at uniform temperature T_∞. We can write the equation of streamlines as $x = \alpha y^{\frac{1}{c}}$, where c is the fraction of the gradient of the stream velocities ($c = \frac{b}{a}$) and α is constant, which gives a particular streamline.

Here for $0 < c \leq 1$ corresponds to the nodal point and $-1 < c \leq 0$ gives saddle stagnation point. The boundary layer flow problem can be express mathematically as

$$\frac{\partial u}{\partial x} + \frac{\partial v}{\partial y} + \frac{\partial w}{\partial z} = 0. \tag{2.2.1}$$

Equation of motion can be written as

$$\frac{d\mathbf{V}}{dt} = \frac{-1}{\rho_{nf}}\nabla.\mathbf{P} + \nu_{nf}\nabla^2\mathbf{V}, \tag{2.2.2}$$

along x-axis

$$u\frac{\partial u}{\partial x} + v\frac{\partial u}{\partial y} + w\frac{\partial u}{\partial z} = ax^2 + \nu_{nf}\frac{\partial^2 u}{\partial z^2}. \tag{2.2.3}$$

along y-axis

$$u\frac{\partial v}{\partial x} + v\frac{\partial v}{\partial y} + w\frac{\partial v}{\partial z} = by^2 + \nu_{nf}\frac{\partial^2 v}{\partial z^2}. \tag{2.2.4}$$

The energy equation can be expressed as

$$u\frac{\partial T}{\partial x} + v\frac{\partial T}{\partial y} + w\frac{\partial T}{\partial z} = \alpha_{nf}\frac{\partial^2 T}{\partial z^2}. \tag{2.2.5}$$

The boundary conditions are given by

$$
\begin{aligned}
u(x,y,z) &= v(x,y,z) = w(x,y,z) = 0 \ \ at \quad z \rightarrow 0,\\
u(x,y,z) &= u_e, \quad v(x,y,z) = v_e \quad when \quad z \rightarrow \infty,\\
T(x,y,z) &= T_s, \quad at\ z \rightarrow 0,\\
T(x,y,z) &= T_\infty \quad when \quad z \rightarrow \infty.
\end{aligned} \tag{2.2.6}
$$

Non dimensionalizing the above equations (2.2.2) to (2.2.5) and their boundary conditions (2.2.6) using the transformations

$$
\begin{aligned}
\eta &= z(\frac{a}{\nu_f})^{\frac{1}{2}},\\
u(x,y,z) &= axf'(\eta), \quad v(x,y,z) = byg'(\eta),\\
w(x,y,z) &= -(a\nu_f)^{\frac{1}{2}}(f+cg) \ \ and \ \ \theta(\eta) = \frac{(T-T_\infty)}{(T_s-T_\infty)}.
\end{aligned} \tag{2.2.7}
$$

The reduced equations are

$$
\frac{\nu_{nf}}{\nu_f}f''' + (f+cg)f'' - f'^2 + 1 = 0, \tag{2.2.8}
$$

$$
\frac{\nu_{nf}}{\nu_f}g''' + (f+cg)g'' + c(1-g'^2) = 0, \tag{2.2.9}
$$

$$
\frac{\alpha_{nf}}{\nu_f}\theta'' + (f+cg)\theta' = 0, \tag{2.2.10}
$$

$$
\begin{aligned}
f(0) &= 0, \ \ f'(0) = 0,\\
g(0) &= 0, \ \ g'(0) = 0,\\
f'(\infty) = 1, \ \ g'(\infty) = 1, \ \ \theta'(\infty) &= 0.
\end{aligned} \tag{2.2.11}
$$

As stated in [39] we have taken the following physical quantities

$$\begin{aligned}
\nu_{nf} &= \frac{\mu_{nf}}{\rho_{nf}} = \frac{\mu_f}{(1-\phi)^{2.5}[(1-\phi)\rho_f+\phi\rho_p]}, \\
\rho_{nf} &= (1-\phi)\rho_f+\phi\rho_p, \\
\mu_{nf} &= \frac{\mu_f}{(1-\phi)^{2.5}}, \qquad \alpha_{nf} = \frac{k_{nf}}{(\rho C_p)_{nf}}, \\
(\rho C_p)_{nf} &= (1-\phi)(\rho C_p)_f+\phi(\rho C_p)_p, \\
\frac{k_{nf}}{k_f} &= \frac{(k_p+2k_f)-2\phi(k_f-k_p)}{(k_s+2k_f)+\phi(k_f-k_p)}.
\end{aligned} \tag{2.2.12}$$

In which (ν_{nf}) represent the kinematic viscosity, (μ_{nf}) indicate viscosity, (ρ_{nf}) is the density, ($(\rho C_p)_{nf}$) shows the specific heat, and (α_{nf}) is the thermal diffusivity of nanofluid, whereas thermal conductivities are k_p, k_f of nanoparticles and base fluid with ρ_p and ρ_f are their densities. The non-dimensional surface drag and rate of heat exchange are chosen as

$$\begin{aligned}
C_{f_x} &= \frac{\tau_{wx}}{\rho_f u_w^2}, \quad C_{f_y} = \frac{\tau_{wy}}{\rho_f u_w^2}, \\
N_{u_x} &= \frac{x q_w}{k_f(T_w-T_\infty)},
\end{aligned} \tag{2.2.13}$$

where q_w, τ_{wx} and τ_{wy} are the heat flux and and wall shear stresses along x- and y-axis, which can be define as

$$\begin{aligned}
q_w &= -k_{nf}\left(\frac{\partial T}{\partial z}\right)_{z=0} \tau_{wx} = \mu_{nf}\left(\frac{\partial u}{\partial z}\right)_{z=0}, \\
\tau_{wy} &= \mu_{nf}\left(\frac{\partial v}{\partial z}\right)_{z=0}.
\end{aligned} \tag{2.2.14}$$

Using transformation (2.2.7), the above equations (2.2.13) and (2.2.14) reduce to the following equations

$$
\begin{aligned}
R_{e_x}^{1/2} C_{f_x} &= \frac{1}{(1-\phi)^{2.5}} f''(0), \\
R_{e_x}^{1/2} C_{f_y} &= \frac{c(y/x)}{(1-\phi)^{2.5}} g''(0), \\
R_{e_x}^{-1/2} N_{u_x} &= -\frac{k_{nf}}{k_f} \theta'(0).
\end{aligned}
\tag{2.2.15}
$$

We have observed the impact of volume fraction and different nanoparticles on velocities and temperature fields for both saddle and nodal points at $Pr = 6.2$, which are shown in the following graphs. Similarly, the streamlines pattern for both the critical points is shown in figure 2.7 and 2.8.

2.3 Discussion

We have solved the system of coupled nonlinear differential equations (2.2.8) to (2.2.10) with boundary conditions (2.2.11) utilizing Runge-Kutta-Fehlberg method. The influence of nanoparticles and its volume fraction (ϕ) ranges from (0 to 0.2) on velocities and temperature fields are shown in the figures (2.1 - 2.6). We have concluded that in figures 2.1 and 2.2, the velocity profiles $f'(\eta)$ along x-axis and $g'(\eta)$ along the y-axis show lessen behavior for the increasing value of ϕ (volume fraction) of nanoparticle. The improvement in temperature with respect to volume fraction parameter ϕ can be seen from 2.3.

Figures 2.4, 2.5 and 2.6 display the effect of different nanoparticles (i.e., Cu, Al_2O_3 and TiO_2) on velocities and temperature at both the critical points, i.e., at $c = 0.5$ and $c = -0.5$, it can be observed that in figure 2.4 and 2.5, the velocity components gives higher values for copper/water and smaller values for alumina/water. In figure 2.6, the behavior of temperature field is maximum for Cu/water and minimum for Al_2O_3/water.

In Table 2.2, the variation in the skin-friction coefficient and the local Nusselt number for different nanoparticles due to the alteration in volume fraction ϕ at the nodal point ($c = 0.5$) is shown. We have listed their numerical results utilizing the shooting method, combine with Runge-Kutta-Fehlberg technique. We can observe the variation by changing nanoparticle volume fraction.

We have discussed three distinct nanoparticles, i.e. copper, titania, and alumina, for all these nanoparticles it is noted that the wall friction coefficient along x- and y-axis enhances as the volume fraction of nanoparticle rises, similarly the heat transfer rate also improves as the volume fraction parameter raises. It is observed that the improvement in Nusselt number is higher for copper and remain at lower levels for titania nanoparticle. As the ability of copper to conduct heat is greater than that of aluminum, but it does not have the capacity to exchange heat faster than aluminum. Even though, for increasing values of nanoparticle volume fraction transfer rate thermal energy increase for the case of the copper nanoparticle. From the Table 2.1 according to (Yazdi et al. [40]), it can be seen that titania nanoparticle has the lowest value of thermal conductivity as compared to copper and alumina that is why lower heat transfer rate can be detected with respect to titania.

Table 2.1: Physical properties of fluid and nanoparticles

Thermophysical properties	Fluid phase(water)	Cu	TiO_2	Al_2O_3
$C_p(J/kgK)$	4179	385	686.2	765
$\rho(kg/m^3)$	997.1	8933	4250	3970
$k(W/mK)$	0.613	400	8.9538	40
$\alpha \times 10^7(m^2/s)$	1.47	1163.1	30.7	131.7

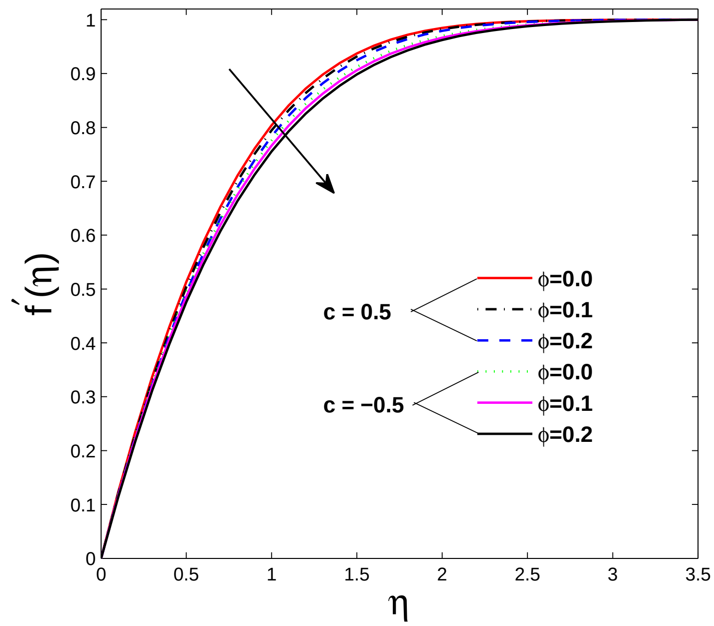

Figure 2.1: Impact of volume fraction on velocity of alumina water nanofluid.

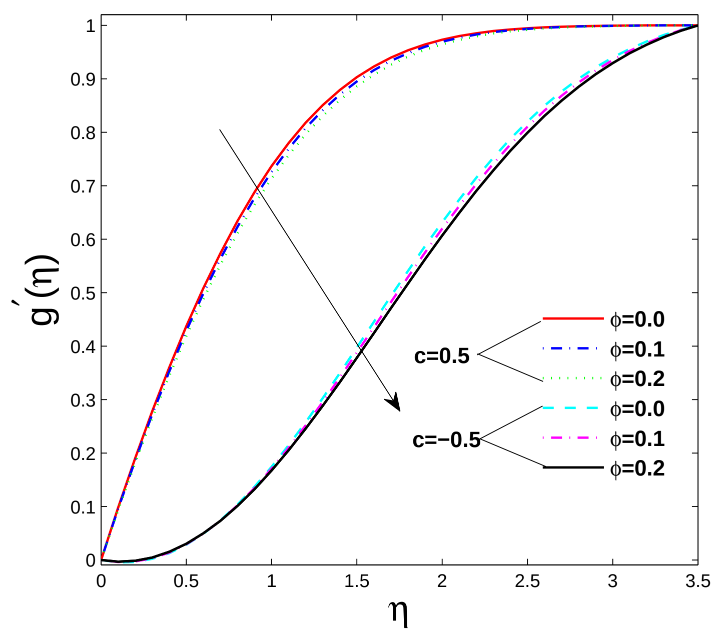

Figure 2.2: Effect of volume fraction on velocity of alumina water nanofluid.

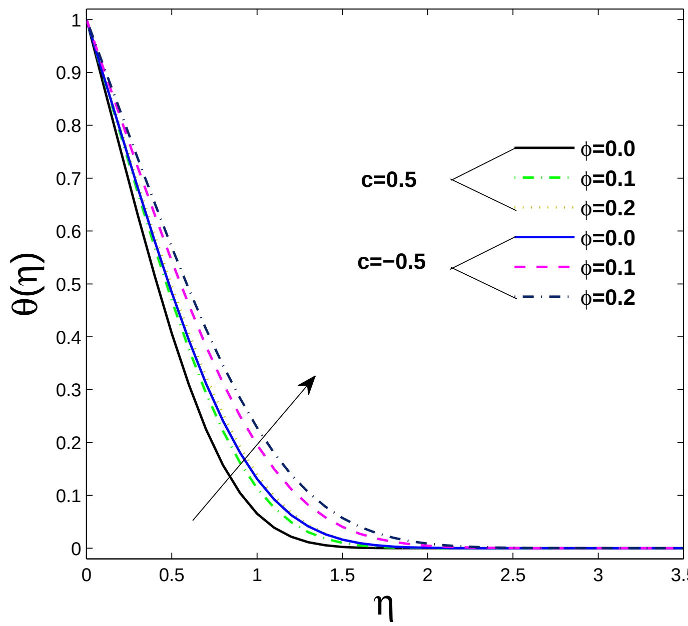

Figure 2.3: Influence of volume fraction on temperature of alumina water nanofluid.

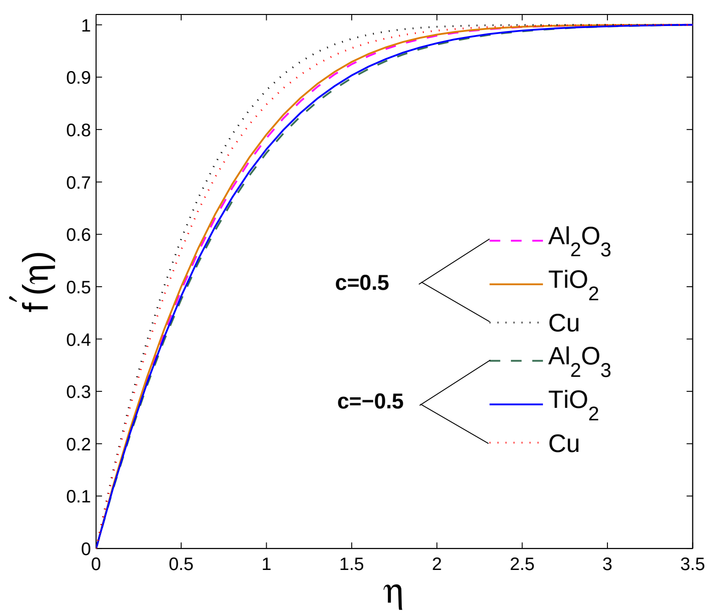

Figure 2.4: Change in $f'(\eta)$ with respect to different nanoparticles.

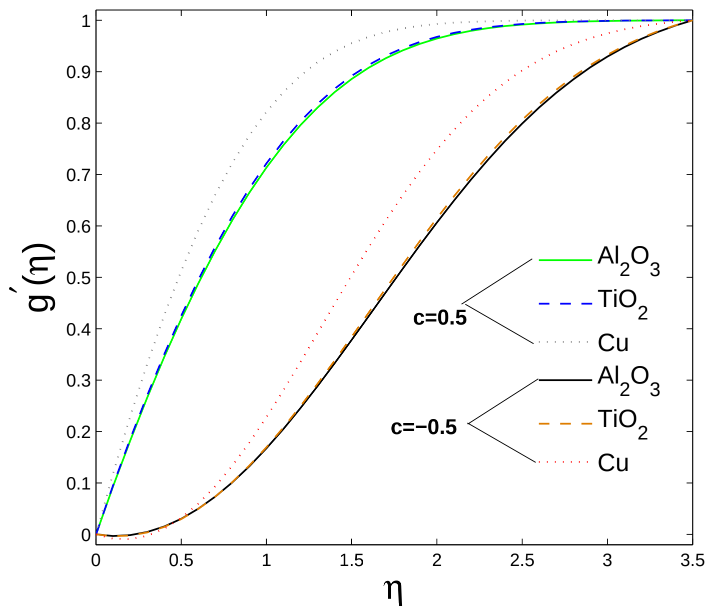

Figure 2.5: Variations in $g'(\eta)$ along different nanoparticles.

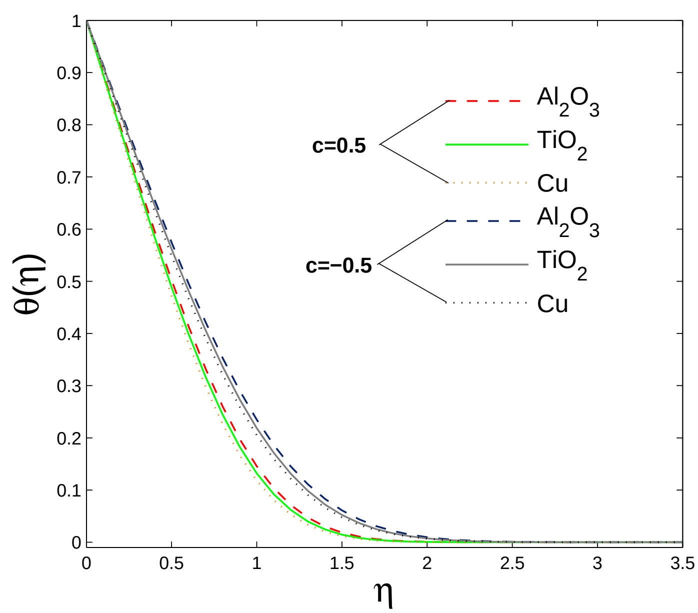

Figure 2.6: Alteration in $\theta(\eta)$ affect by different nanoparticles.

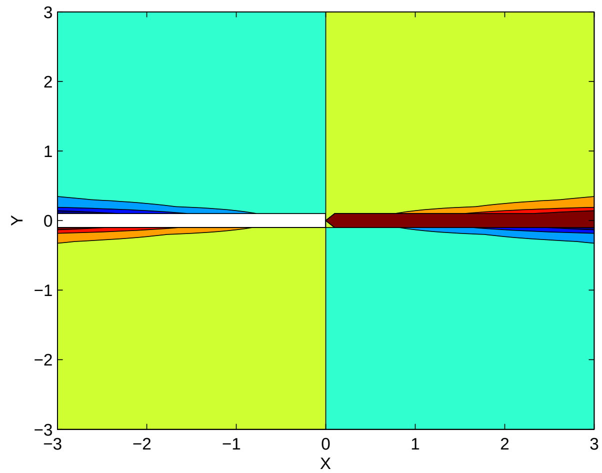

Figure 2.7: Streamlines pattern at nodal stagnation point

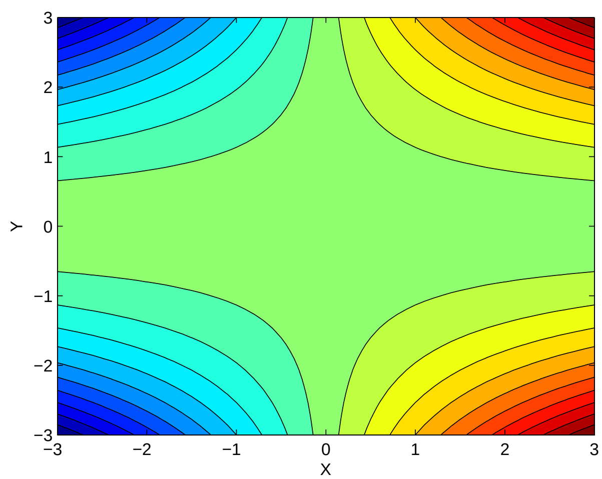

Figure 2.8: streamlines pattern at saddle stagnation point

Table 2.2: The impact of volume fraction (ϕ) of different nanoparticle on wall stresses along x- and y-axis, and rate of heat transfer for different nanoparticles at nodal stagnation point, when $Pr = 6.2$.

Nanoparticles	ϕ	$R_{e_x}^{1/2} C_{f_x}$	$R_{e_x}^{1/2} C_{f_y}$	$R_{e_x}^{-1/2} N_{u_x}$
		Numerical	Numerical	Numerical
Cu	0.0	1.5254	0.6357	1.4348
	0.1	1.9367	0.7630	1.6179
	0.2	2.6985	1.0619	1.9290
	0.3	3.6417	1.4346	2.2474
	0.4	4.9072	1.9331	2.5876
TiO_2	0.0	1.5254	0.6357	1.4348
	0.1	1.6642	0.6556	1.4953
	0.2	2.1524	0.8480	1.6906
	0.3	2.7832	1.0964	1.8820
	0.4	3.6424	1.4350	2.0713
Al_2O_3	0.0	1.5254	0.6357	1.4348
	0.1	1.6466	0.6487	1.5292
	0.2	2.1155	0.8334	1.7670
	0.3	2.7234	1.0728	2.0125
	0.4	3.5525	1.3996	2.2719

2.4 Closing comments

We have reviewed the flow of nanofluid along stagnation point over a circular cylinder with wavy radius, the problem is then solved by the numerical approach. Three types of nanoparticle are under our observation with water, we got the following remarks from our study.

★ Discussing nanofluid with alumina nanoparticle we have checked that by enhancing the value of nanoparticle volume fraction the components of velocity along x- and y-axis show a decreasing behavior for the critical points.

★ It is observed that at both the nodal and saddle stagnation point the temperature field increases as the volume fraction ϕ raises.

★ The behavior of the increasing velocity component for both $c = 0.5$ and $c = -0.5$ have the highest value for copper water and lower for alumina water nanofluid.

★ By raising volume fraction of nanoparticle the surface friction and rate of heat exchange for the considered nanoparticle increases.

★ At the surface the Nusselt number and skin friction drag shows highest values for Cu-water nanofluid as compared to titania and alumina-water nanofluid.

★ From the study, we have an access to the fact that Cu-nanoparticles potentially useful in the enhancement of heat transfer.

Chapter 3

Magneto-hydrodynamics steady three dimensional stagnation point flow of a nanofluid past a circular cylinder

3.1 Preamble

The aim of this chapter is to indicate the steady flow of a nanofluid in three dimensions passed over a cylinder under the action of the induced magnetic field. The Navier-Stokes and energy equations of this boundary-layer problem are transmuted into nonlinear differential equations by applying some transformations. The reduced problem is utilized numerically by shooting method along with Runge-Kutta-Fehlberg method. The flow is examined in the neighborhood of critical points. We have scrutinized nanofluid with nanoparticles (Cu, Al_2O_3, TiO_2) and base fluid (water) in this article. We have investigated that the fluid velocity increases with the increment in nanoparticle volume fraction (ϕ), similarly there is a rise in the velocity field of nanofluid for all nanoparticles taken in the study. The effect of a magnetic parameter (β), magnetic Prandtl number (M) on the velocity and temperature profiles has been discussed and analyzed. Moreover, the friction drag and rate of heat transfer vary at the surface for different nanoparticles and distinct parameters have been discussed, and their numerical results are listed in the last three tables.

3.2 Mathematical Formulation

We are considering the surface at $z = 0$ and the fluid at $z \geq 0$. First, we are assuming the flow near A, which is a nodal stagnation point with a maximum radius. The reference system is chosen such that the y-axis is along the surface and z-axis normal to it while x- axis is taken in its upward direction. Howarth [38] initiated the velocity components near stagnation point A as $u_e = ax$, $v_e = by$, a and b are constants which represent velocity with $|a| \geq |b|$, $a > 0$, so $b = 0$ The diagram of the cylinder and streamlines pattern on the cylinder are given in Figure 3.1.

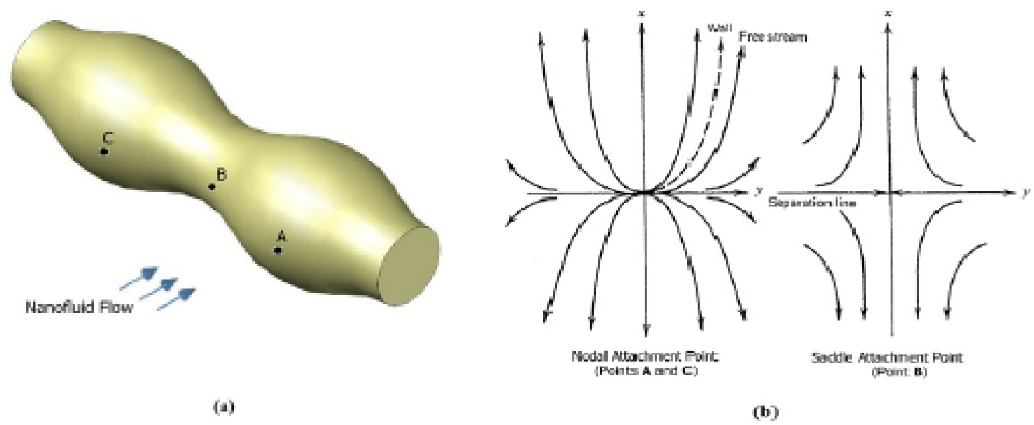

(a) Diagram of flow around cylinder (b) Streamlines patterns on the cylinder

Figure 3.1: Physical sketch of flow analysis

In the external flow, the streamlines equation is given by $x = \alpha y^{\frac{1}{c}}$, where c is the fraction of the gradient of the stream velocities ($c = \frac{b}{a}$) and α is constant, which gives a particular streamline. So if $0 < c \leq 1$ we have a nodal stagnation point, whereas $-1 < c \leq 0$ represent saddle stagnation point, while $c = 0$ corresponds to the plane flow. Besides this we are analyzing the flow under the action of the uniform magnetic field with constant strength H_0 which is applied outside of the boundary layer with components (H_1, H_2, H_3) along x, y and z-direction. H_3 vanishes at the surface while H_1 and H_2 approaches to the values $H_e(x)$ and $H_e(y)$ at the boundary layer. The surface is maintained at a constant temperature T_w while the external flow has an ambient uniform temperature T_∞. The governing boundary layer equations are as follow

$$\frac{\partial u}{\partial x} + \frac{\partial v}{\partial y} + \frac{\partial w}{\partial z} = 0, \tag{3.2.1}$$

$$\frac{\partial H_1}{\partial x} + \frac{\partial H_2}{\partial y} + \frac{\partial H_3}{\partial z} = 0, \tag{3.2.2}$$

$$\begin{aligned} u\frac{\partial u}{\partial x} + v\frac{\partial u}{\partial y} + w\frac{\partial u}{\partial z} - \frac{\mu_e}{4\pi\rho_{nf}}\left(H_1\frac{\partial H_1}{\partial x} + H_2\frac{\partial H_1}{\partial y} + H_3\frac{\partial H_1}{\partial z}\right) \\ = ax^2 - \frac{\mu_e}{4\pi\rho_{nf}}H_e(x)\frac{dH_e(x)}{dx} + \nu_{nf}\frac{\partial^2 u}{\partial z^2}, \end{aligned} \tag{3.2.3}$$

$$\begin{aligned} u\frac{\partial v}{\partial x} + v\frac{\partial v}{\partial y} + w\frac{\partial v}{\partial z} - \frac{\mu_e}{4\pi\rho_{nf}}\left(H_1\frac{\partial H_2}{\partial x} + H_2\frac{\partial H_2}{\partial y} + H_3\frac{\partial H_2}{\partial z}\right) \\ = by^2 - \frac{\mu_e}{4\pi\rho_{nf}}H_e(y)\frac{dH_e(y)}{dy} + \nu_{nf}\frac{\partial^2 v}{\partial z^2}, \end{aligned} \tag{3.2.4}$$

$$\begin{aligned} u\frac{\partial H_1}{\partial x} + v\frac{\partial H_1}{\partial y} + w\frac{\partial H_1}{\partial z} - H_1\frac{\partial u}{\partial x} - H_2\frac{\partial u}{\partial y} - H_3\frac{\partial u}{\partial z} \\ = \eta_0\frac{\partial^2 H_1}{\partial z^2}, \end{aligned} \tag{3.2.5}$$

$$u\frac{\partial H_2}{\partial x} + v\frac{\partial H_2}{\partial y} + w\frac{\partial H_2}{\partial z} - H_1\frac{\partial v}{\partial x} - H_2\frac{\partial v}{\partial y} - H_3\frac{\partial v}{\partial z} = \eta_0\frac{\partial^2 H_2}{\partial z^2}, \tag{3.2.6}$$

$$u\frac{\partial T}{\partial x} + v\frac{\partial T}{\partial y} + w\frac{\partial T}{\partial z} = \alpha_{nf}\frac{\partial^2 T}{\partial z^2}, \tag{3.2.7}$$

The partial slip boundary conditions for velocity, and temperature jump condition are stated as

$$\begin{aligned} u = U_w + N_1\mu_{nf}\frac{\partial u}{\partial z}, \quad v = V_w + N_1\mu_{nf}\frac{\partial v}{\partial z}, \quad w = 0, \\ \frac{\partial H_1}{\partial z} = \frac{\partial H_2}{\partial z} = H_3 = 0, \\ T = T_w + N_2 k_{nf}\frac{\partial T}{\partial z}, \quad at \quad z = 0, \\ u \to u_e, \quad v \to v_e, \quad T \to T_\infty, \\ H_1 \to H_e(x), \quad H_2 \to H_e(y), \quad as \quad z \to \infty, \end{aligned} \tag{3.2.8}$$

here U_w, V_w, N_1 and N_2 are the wall velocities and slip parameters, $H_e(x) = xH_0$ and $H_e(y) = yH_0$ are the x- and y-magnetic fields at the boundary layer. The other quantities like ν_{nf}, ρ_{nf}, μ_{nf} and α_{nf}, $(\rho C_p)_{nf}$ and k_{nf} are the kinematic viscosity, density, viscosity and thermal diffusivity of corresponding nanofluid, can be identified according to [40].

$$\begin{aligned} \nu_{nf} = \frac{\mu_f}{(1-\phi)^{2.5}[(1-\phi)\rho_f + \phi\rho_s]}, \\ \rho_{nf} = (1-\phi)\rho_f + \phi\rho_s, \\ \mu_{nf} = \frac{\mu_f}{(1-\phi)^2.5}, \qquad \alpha_{nf} = \frac{k_{nf}}{(\rho C_p)_{nf}}, \\ (\rho C_p)_{nf} = (1-\phi)(\rho C_p)_f + \phi(\rho C_p)_s, \\ \frac{k_{nf}}{k_f} = \frac{(k_s + 2k_f) - 2\phi(k_f - k_s)}{(k_s + 2k_f) + \phi(k_f - k_s)}. \end{aligned} \tag{3.2.9}$$

Here ϕ is the nanoparticle volume fraction, k_s, k_f, ρ_s and ρ_f are the thermal conductivities and densities of the fluid and solid fractions. Non-dimensionalizing using

$$\begin{aligned}
\eta = z(\frac{a}{\nu_f})^{\frac{1}{2}} \quad u = axf'(\eta), \\
v = byg'(\eta), \quad w = -(a\nu_f)^{\frac{1}{2}}(f+cg), \\
H_1 = xH_0h_1'(\eta), \quad H_2 = yH_0h_2'(\eta), \\
H_3 = -(\frac{\nu_f}{a})^{\frac{1}{2}}H_0(h_1+h_2), \quad \theta(\eta) = \frac{(T-T_\infty)}{(T_w-T_\infty)}.
\end{aligned} \tag{3.2.10}$$

Equations (3.2.3) to (3.2.7) along with the double slip boundary conditions (3.2.8), take the form

$$\frac{\nu_{nf}}{\nu_f}f''' + (f+cg)f'' - f'^2 + 1 - \beta\frac{\rho_f}{\rho_{nf}}\left(1 - h_1'^2 + (h_1+h_2)h_1''\right) = 0, \tag{3.2.11}$$

$$\frac{\nu_{nf}}{\nu_f}g''' + (f+cg)g'' + c(1-g'^2) - c\beta\frac{\rho_f}{\rho_{nf}}\left(1 - h_1'^2 + (h_1+h_2)h_1''\right) = 0, \tag{3.2.12}$$

$$h_1''' + M(f+cg)h_1'' - M(h_1+h_2)f'' = 0, \tag{3.2.13}$$

$$h_2''' + M(f+cg)h_2'' - Mc(h_1+h_2)g'' = 0, \tag{3.2.14}$$

$$\frac{\alpha_{nf}}{\nu_f}\theta'' + (f+cg)\theta' = 0, \tag{3.2.15}$$

$$\begin{aligned}
f(0) = 0, \quad f'(0) - \frac{\mu_{nf}}{\mu_f}\delta_1 f''(0) = 0, \quad g(0) = 0, \\
g'(0) - \frac{\mu_{nf}}{\mu_f}\delta_1 g''(0) = 0, \quad h_1(0) = 0, \quad h_1''(0) = 0, \\
h_2(0) = 0, \quad h_2''(0) = 0, \quad \theta(0) - \frac{k_{nf}}{k_f}\delta_2\theta'(0) = 1, \\
f'(\infty) = 1, \;\; g'(\infty) = 1, \;\; h_1'(\infty) = 1, \\
h_2'(\infty) = 1, \quad \theta'(\infty) = 0.
\end{aligned} \tag{3.2.16}$$

In which δ_1 and δ_2 are the corresponding velocity and thermal slip parameter, whereas β and M can be written as

$$\beta = \frac{\mu_e}{4\pi\rho_f}\left(\frac{H_0}{a}\right)^2, \quad and \;\; M = \frac{\nu_f}{\eta_0}. \tag{3.2.17}$$

Here μ_e and η_0 are the magnetic permeability and magnetic diffusivity. The non-dimensional form of surface drag and rate of heat transfer can be expressed as wall-friction coefficients (C_{f_x}, C_{f_y}), and Nusselt number, which can be written as

$$\begin{aligned} C_{f_x} &= \frac{\tau_{wx}}{\rho_f u_w^2}, C_{f_y} = \frac{\tau_{wy}}{\rho_f u_w^2}, \\ N_{u_x} &= \frac{x q_w}{k_f(T_w - T_\infty)}. \end{aligned} \tag{3.2.18}$$

Where q_w, τ_{wx} and τ_{wy} are the wall heat flux and shear forces at the surface, these are given by the following equations.

$$\begin{aligned} \tau_{wx} = \mu_{nf}\left(\frac{\partial u}{\partial z}\right)_{z=0}, \quad \tau_{wy} &= \mu_{nf}\left(\frac{\partial v}{\partial z}\right)_{z=0}, \\ q_w &= -k_{nf}\left(\frac{\partial T}{\partial z}\right)_{z=0}, \end{aligned} \tag{3.2.19}$$

simplifying these using the transformations (3.2.10) we get the following dimensionless forms of skin friction and rate of heat transfer

$$\begin{aligned} R_{e_x}^{1/2} C_{f_x} &= \frac{1}{(1-\phi)^{2.5}} f''(0), \\ R_{e_x}^{1/2} C_{f_y} &= \frac{c(y/x)}{(1-\phi)^{2.5}} g''(0), \\ R_{e_x}^{-1/2} N_{u_x} &= -\frac{k_{nf}}{k_f}\theta'(0). \end{aligned} \tag{3.2.20}$$

3.3 Discussion

Under the similarity transformations (3.2.10) the equations of the conservation of momentum, induced magnetic field and energy equation are reduced into a system of coupled non-linear differential equations (3.2.11 to 3.2.15) with the boundary conditions (3.2.16). These expressions are solved by using shooting technique along with Runge-Kutta-Fehlberg scheme. The impact of volume fraction ϕ and different parameters, i.e., β, M, $\delta 1$ and $\delta 2$ on velocity profiles, magnetic field and temperature are discussed through graphs. Here we have considered three types of different nanoparticles, i.e., copper (Cu), titania (TiO_2) and alumina (Al_2O_3). Implementing thermophysical properties form Table 3.1, each case of nanofluid has been utilized. Selecting the values of parameters as, $\beta < 1$, $M \leq 1$, $Pr = 6.2$ and $o \leq \phi \leq 0.2$. Analysis has been carried out for copper-water nanofluid. Figures 3.4, 3.5, 3.6, 3.7 and 3.8 shows the impact of volume fraction (ϕ) of nanoparticle on velocity fields, induced magnetic-field components and temperature. It is noted that by increasing volume fraction (ϕ) of copper nanoparticle the velocity fields ($f'(\eta)$, $g'(\eta)$), magnetic-field components ($h_1'(\eta)$, $h_2'(\eta)$) and temperature profile ($\theta(\eta)$), also increases along the nodal and saddle stagnation points. Figures 3.9, 3.10 and 3.11 are plotted for the behavior of different nanoparticles on velocity and temperature profile at $c = 0.1$ and $c = -0.1$, and it is observed that in figures 3.9 and 3.10 the velocity profiles have higher values for Cu nanoparticles and smaller values for Al_2O_3 nanoparticles, while in figure 3.11 the results are reversed for copper/water and alumina/water nanofluids they have minimum and maximum temperature fields. We have also observed the effect of the magnetic parameter β on velocity components and induced magnetic-field components, and the results can be seen from figures 3.12, 3.13, 3.14 and 3.15. From the mentioned figures, it can be noticed that as the magnetic parameter (β) ascents, the corresponding velocity components and the induced magnetic-field components descent. Similarly, the impact of magnetic-Prandtl number M on both the components of the induced magnetic field is sketched in figures 3.16 and 3.17, the graphs show that induced magnetic-field components enhance for the increasing values of magnetic-Prandtl number (M). The variations in velocity components ($f'(\eta)$, $g'(\eta)$) and temperature field ($\theta(\eta)$) with respect to the velocity slip parameter δ_1 and thermal slip parameter δ_2 can be seen from the figures 3.18, 3.19 and 3.20. It can be detected from the figures that the velocity components rise with the increase in δ_1 whereas the temperature field falls with the increment in δ_2. The streamlines pattern at nodal and saddle stagnation points has been sketched in 3.2 and 3.3. The variation in skin friction coefficients and Nusselt number by cause of changing the emerging parameters can be observed from Tables 3.3, 3.4, 3.5.

Table 3.1: Thermophysical properties of fluid and nanoparticles conforming to (Yazdi et al. [40])

Thermophysical properties	Fluid phase(water)	Cu	TiO_2	Al_2O_3
$C_p(J/kgK)$	4179	385	686.2	765
$\rho(kg/m^3)$	997.1	8933	4250	3970
$k(W/mK)$	0.613	400	8.9538	40
$\alpha \times 10^7(m^2/s)$	1.47	1163.1	30.7	131.7

The effect of volume fraction (ϕ) on dimensionless surface drag and heat flow rate for different nanoparticles at a nodal point, and its comparison with [41] is displayed in Table 3.2.

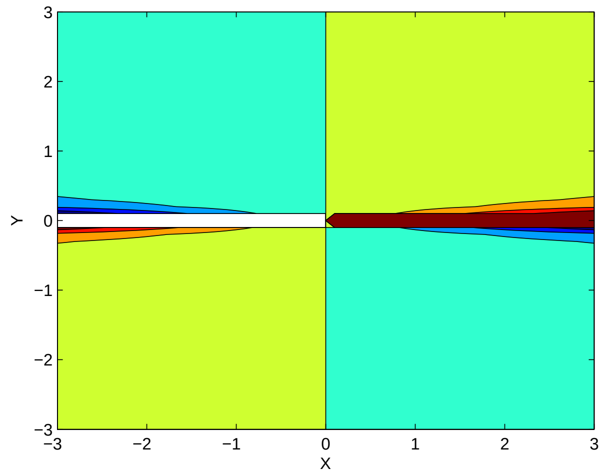

Figure 3.2: Streamlines pattern at the nodal stagnation point for $\alpha = 0$.

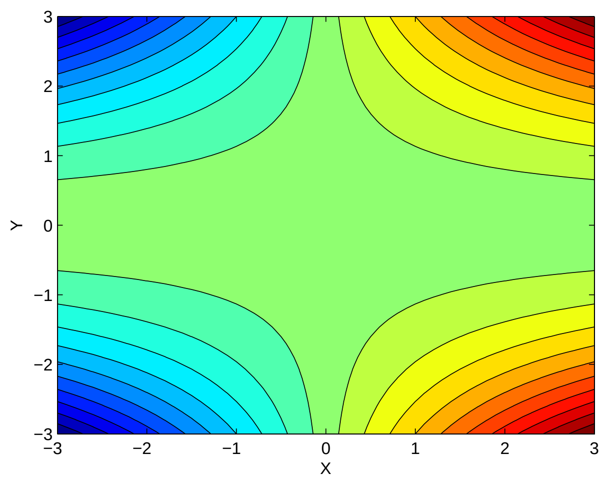

Figure 3.3: Streamlines pattern along the saddle stagnation point for $\alpha = 0$.

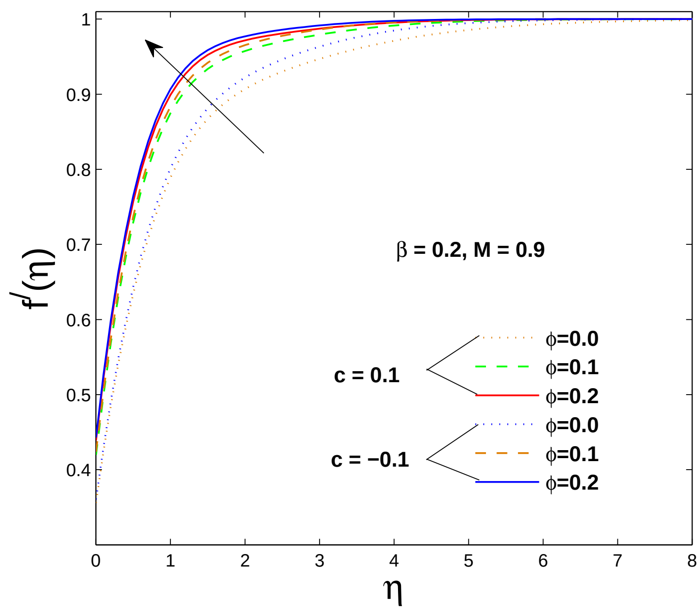

Figure 3.4: Variation in velocity profile along the x-axis caused by changing ϕ.

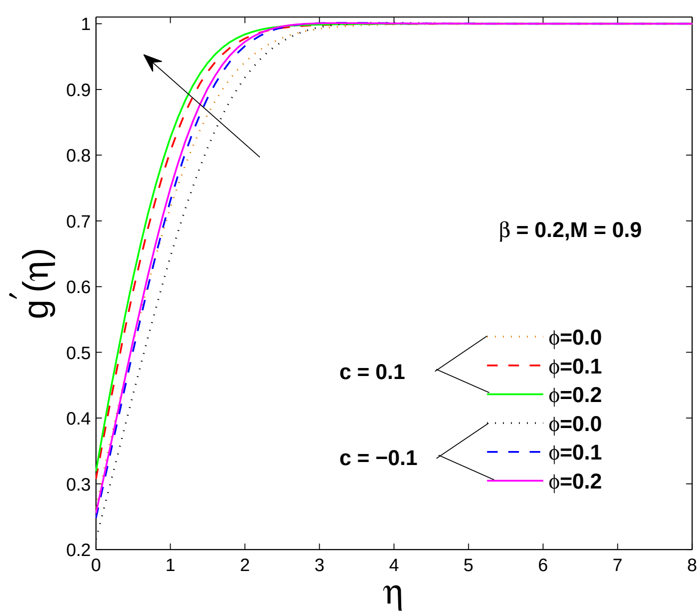

Figure 3.5: Change in velocity profile along the y-axis with respect to volume fraction of nanoparticle.

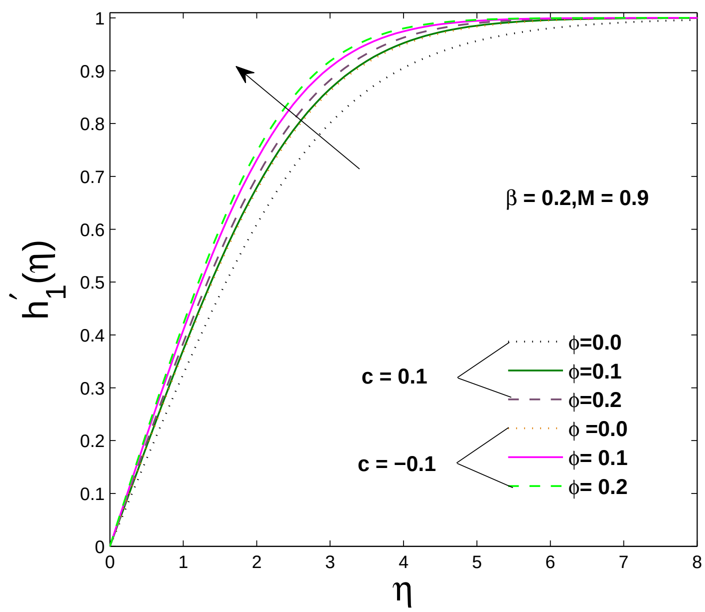

Figure 3.6: Influence of ϕ on induced magnetic field along the x-axis.

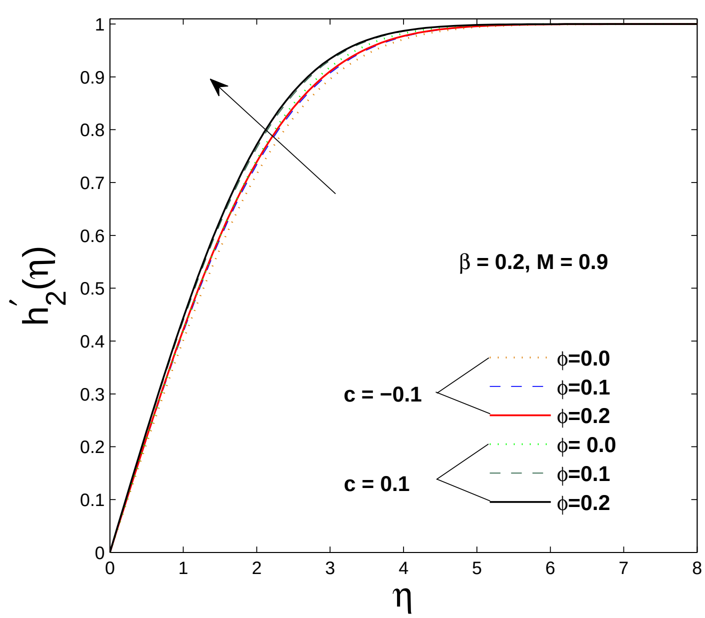

Figure 3.7: Impact of ϕ on induced magnetic field along the y-axis.

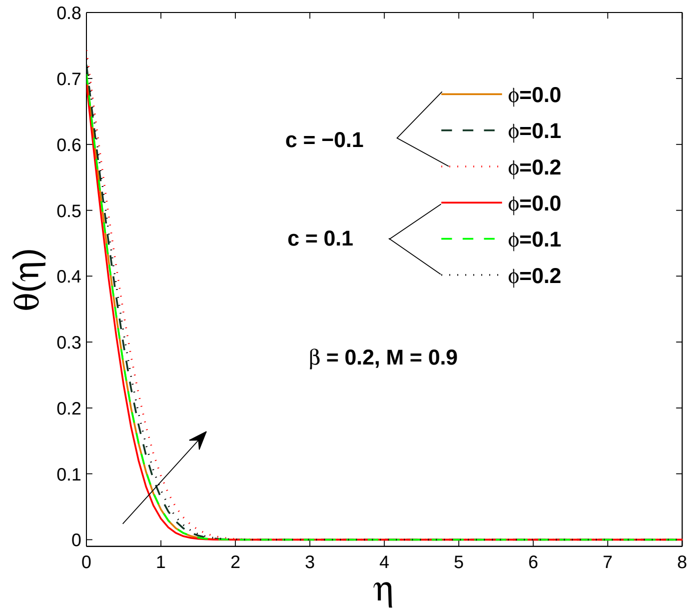

Figure 3.8: Effect of ϕ on temperature profile.

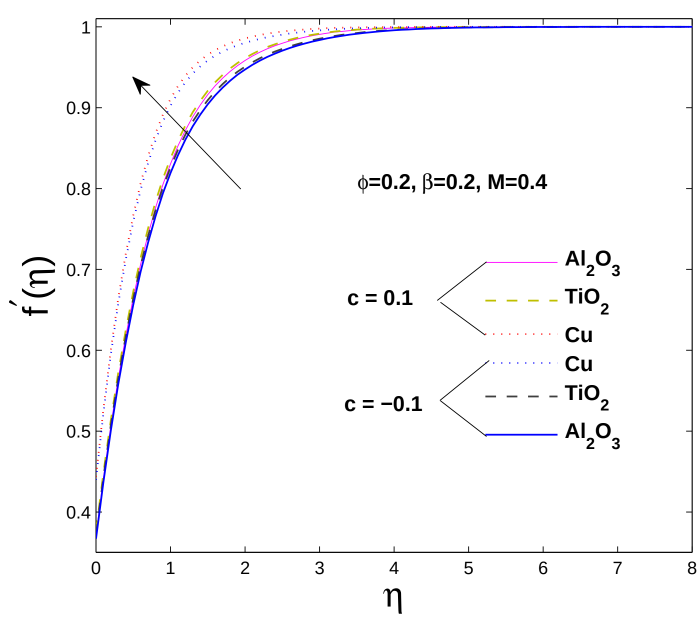

Figure 3.9: Effect of different nanoparticles on velocity profile along the x-axis.

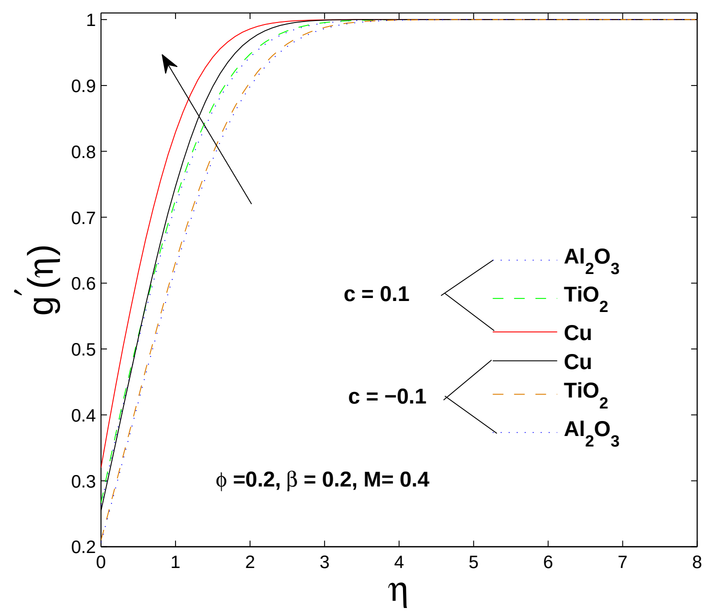

Figure 3.10: Influence of distinct nanoparticles on velocity profile along the y-axis.

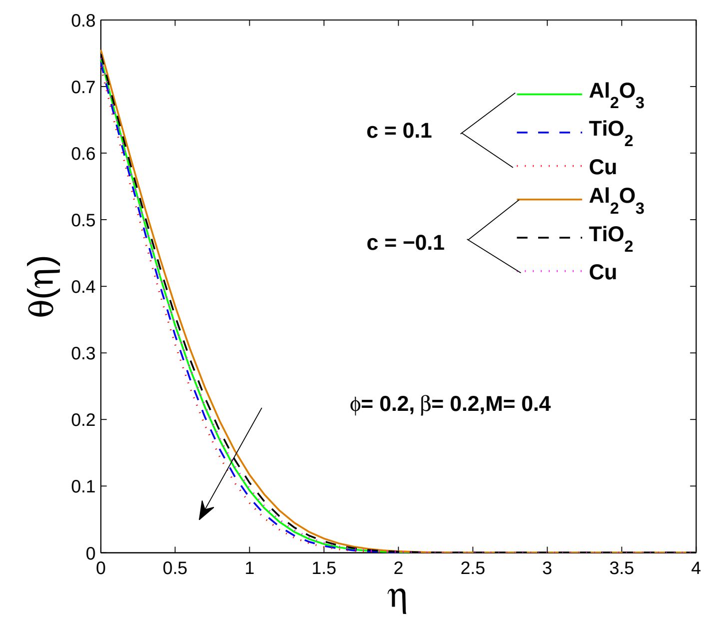

Figure 3.11: Effect of different nanoparticles on temperature.

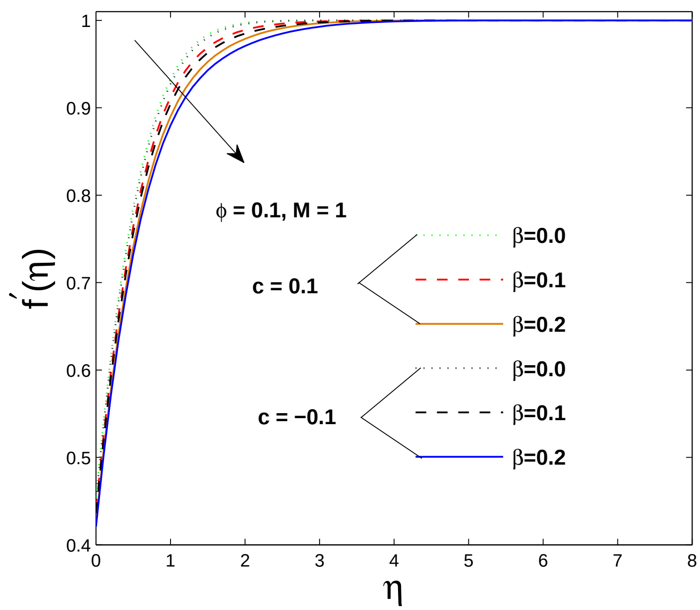

Figure 3.12: Modification in the velocity field ($f'(\eta)$) with respect to magnetic parameter β.

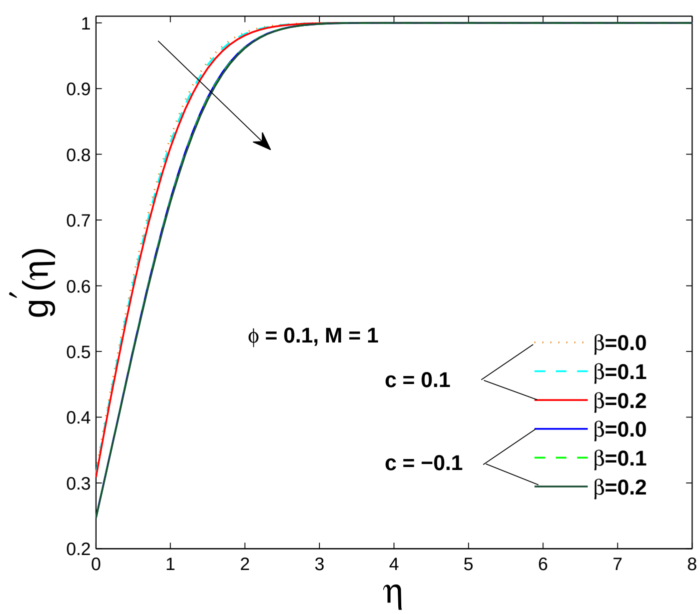

Figure 3.13: Effect of magnetic parameter β on velocity field ($g'(\eta)$).

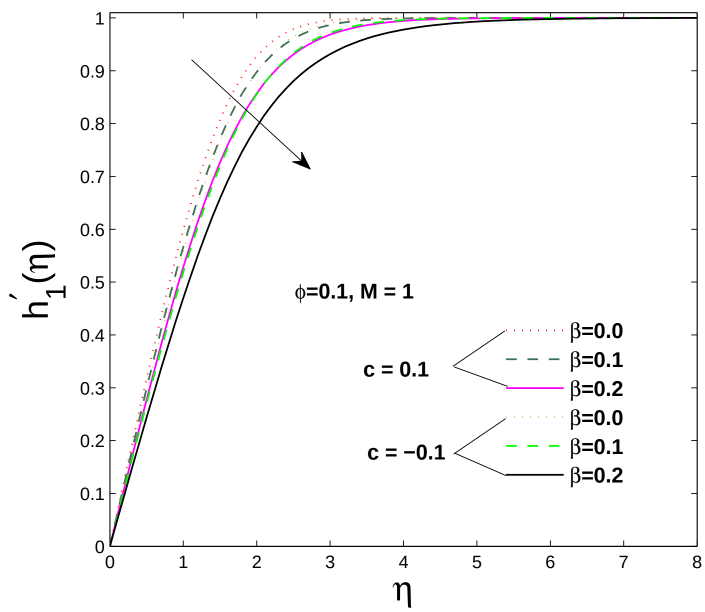

Figure 3.14: Impact of magnetic parameter β on $h_1'(\eta)$.

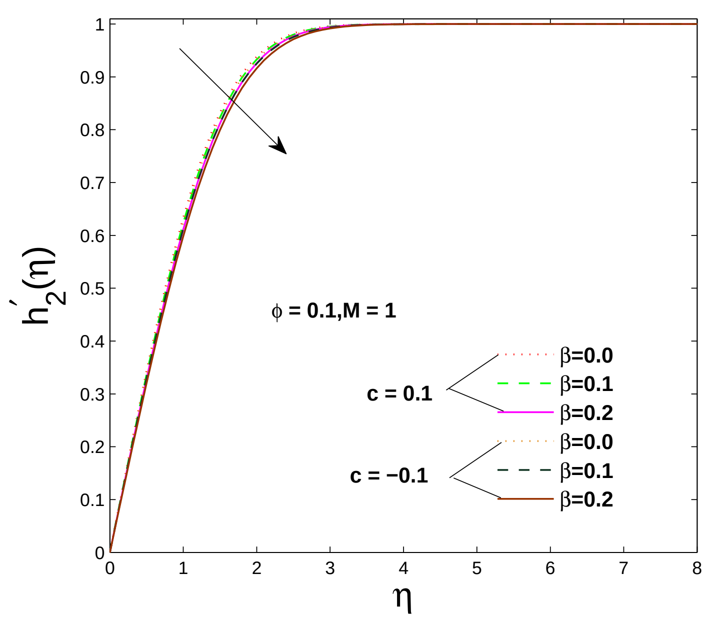

Figure 3.15: Influence of magnetic parameter β on $h_2'(\eta)$.

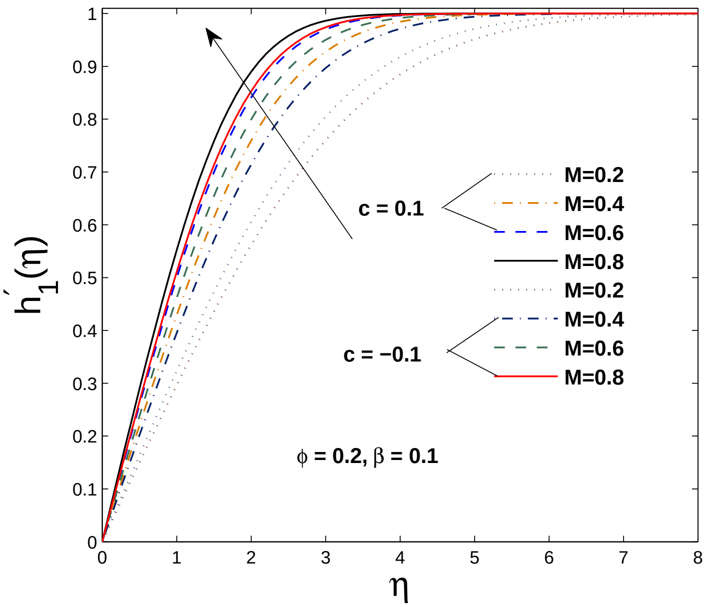

Figure 3.16: Effect of magnetic-Prandtl number M on $h_1'(\eta)$.

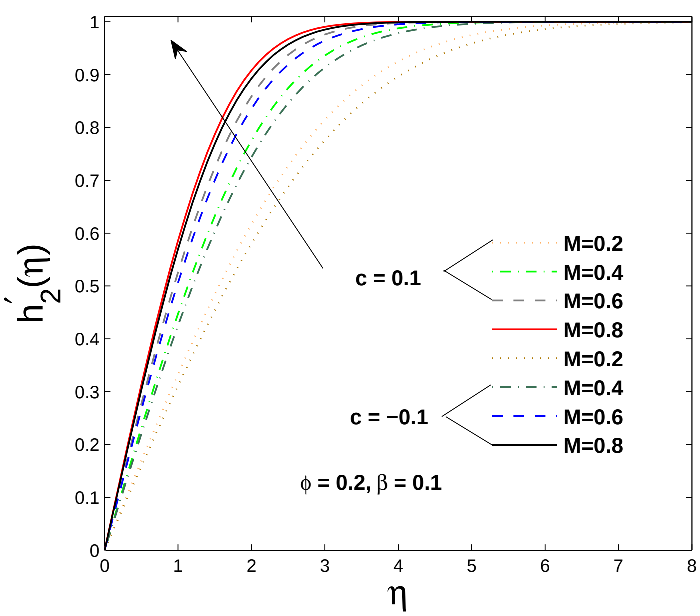

Figure 3.17: Change in $h_2'(\eta)$ affected by magnetic-Prandtl number M.

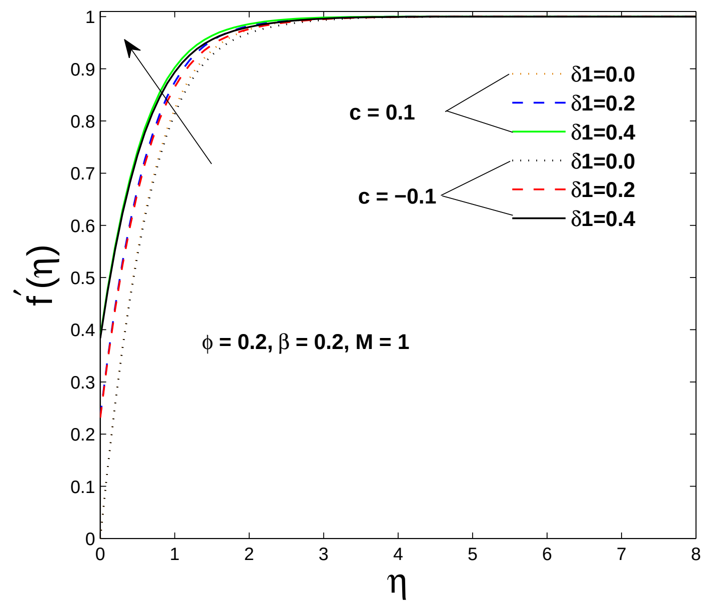

Figure 3.18: Influence of the slip parameter δ_1 on velocity $(f'(\eta))$.

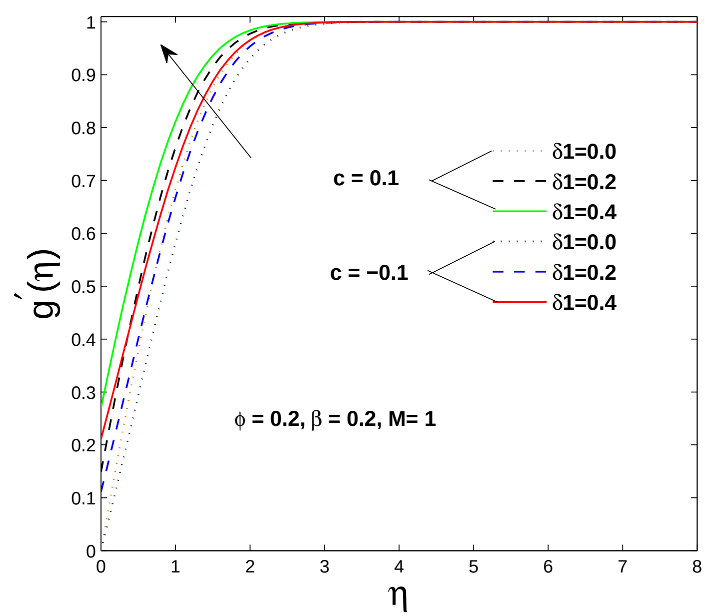

Figure 3.19: Impact of the slip parameter δ_1 on velocity $(g'(\eta))$.

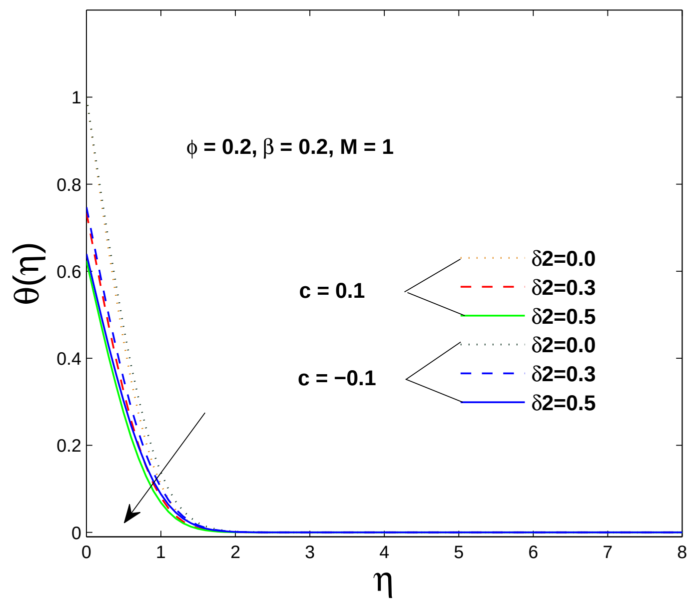

Figure 3.20: Effect of thermal slip parameter δ_2 on temperature field.

Table 3.2: Comparison table for the values of non-dimensional surface drag along x- and y- axis and heat transfer rate varying with volume fraction ϕ at the nodal point, taking $\beta = 0$, $M = 0$, $\delta_1 = 0$ and $\delta_2 = 0$.

Nanoparticles	ϕ	$R_{e_x}^{1/2} C_{f_x}$		$R_{e_x}^{1/2} C_{f_y}$		$R_{e_x}^{-1/2} N_{u_x}$	
		citation	present	citation	present	citation	present
Cu	0.0	1.2380	1.23792	0.0671	0.0670	1.15561	1.15560
	0.1	1.8925	1.8924	0.1025	0.10248	1.4408	1.4407
	0.2	2.2274	2.2273	0.1283	0.1282	1.4961	1.4960
TiO_2	0.0	1.2380	1.23792	0.0671	0.0670	1.15561	1.15560
	0.1	1.6262	1.62624	0.0881	0.0880	1.4010	1.4009
	0.2	2.1033	2.1032	0.1140	0.1139	1.6563	1.6562
Al_2O_3	0.0	1.2380	1.23792	0.0671	0.0670	1.15561	1.15560
	0.1	1.6089	1.60893	0.1120	0.1120	1.3793	1.3792
	0.2	2.0673	2.0672	0.1170	0.11703	1.6087	1.6086

Table 3.3: Data table for skin-friction coefficients and local Nusselt number of copper nanoparticle taking $Pr = 6.2$ and $c = 0.1$.

Nanoparticle	ϕ	β	M	δ_1	δ_2	$R_{e_x}^{1/2} C_{f_x}$	$R_{e_y}^{1/2} C_{f_y}$	$R_{e_x}^{-1/2} N_{u_x}$
	0.0	0.2	0.9	0.4	0.3	0.7796	0.0554	1.0044
	0.1					1.0886	0.0795	1.1917
	0.2					1.3252	0.1008	1.3419
	0.1	0.0	1.0	0.4	0.3	1.1637	0.0819	
		0.1				1.1271	0.0808	
Cu		0.2				1.0891	0.0795	
	0.2	0.2	1.0	0.0	0.3	2.4916	0.1390	
				0.2		1.7710	0.1210	
				0.4		1.3257	0.1009	
	0.2	0.2	1.0	0.4	0.0			2.2467
	0.2				0.3			1.3421
	0.2				0.5			1.1396

Table 3.4: Numerical detail for surface shear stresses and heat transfer rate against distinct parameters for titania nanoparticle.

Nanoparticle	ϕ	β	M	δ_1	δ_2	$R_{e_x}^{1/2}C_{f_x}$	$R_{e_y}^{1/2}C_{f_y}$	$R_{e_x}^{-1/2}N_{u_x}$
	0.0	0.2	0.9	0.4	0.3	0.7796	0.0554	1.0044
	0.1					0.9691	0.0702	1.1127
	0.2					1.1508	0.0858	1.2021
	0.1	0.0	1.0	0.4	0.3	1.0636	0.0731	
		0.1				1.0179	0.0717	
TiO_2		0.2				0.9697	0.0702	
	0.2	0.2	1.0	0.0	0.3	1.9246	0.1095	
				0.2		1.4691	0.0990	
				0.4		1.1515	0.0858	
	0.2	0.2	1.0	0.4	0.0			2.1900
	0.2				0.3			1.3217
	0.2				0.5			1.0454

Table 3.5: Numerical results from the influence of distinct parameters on wall shear stresses and local heat transfer rate for alumina nanoparticle at the nodal point.

Nanoparticle	ϕ	β	M	δ_1	δ_2	$R_{e_x}^{1/2} C_{f_x}$	$R_{e_y}^{1/2} C_{f_y}$	$R_{e_x}^{-1/2} N_{u_x}$
	0.0	0.2	0.9	0.4	0.3	0.7796	0.0554	1.0044
	0.1					0.9606	0.0696	1.1414
	0.2					1.1370	0.0846	1.2658
	0.1	0.0	1.0	0.4	0.3	1.0566	0.0725	
		0.1				1.0102	0.0711	
Al_2O_3		0.2				0.9612	0.0696	
	0.2	0.2	1.0	0.0	0.3	1.8853	0.1075	
				0.2		1.4463	0.0974	
				0.4		1.1376	0.0847	
	0.2	0.2	1.0	0.4	0.0			2.1139
	0.2				0.3			1.2935
	0.2				0.5			1.0277

3.4 Conclusion

In this article, we have studied three specific nanoparticles (alumina (Al_2O_3), titania (TiO_2) and copper (Cu)) with base fluid taken to be water. We have got the following remarks from our study.

- ✠ For nanofluid with copper nanoparticle the velocity components show increasing behavior as the volume fraction of nanoparticle (copper) rises along both the saddle and nodal points.
- ✠ The temperature also improves for the CU-water nanofluid with the enhancement in volume fraction (ϕ) of nanoparticle along stagnation points
- ✠ It is noted that for all three nanoparticles, alumina and copper have the smaller and higher velocities components.
- ✠ The effect of a magnetic parameter (β) on skin friction coefficients has been examined, and it is noted that shear stresses at the surface reduce as (β) rise.
- ✠ We have observed that for considered nanoparticles the skin friction coefficients, and local Nusselt number expand for the increasing values of ϕ.
- ✠ We have remarked that there is fall in wall shear stresses and rate of heat transfer when velocity and thermal slip parameters raise.
- ✠ The surface shear stresses and heat transfer rate have higher values for copper-water nanofluid as compared to titania and alumina-water nanofluids.

Bibliography

[1] D. Rouson, S. Kassinos, I. Sarris, and F. Toschi. Particle dispersion in magnetohydrodynamic turbulence at low magnetic reynolds number. *Center for Turbulence Research Proceedings of the Summer Program (IV. MAGNETOHYDRODYNAMICS)*, 2006.

[2] T. Hartlep, M. S. Miesch, and N. N. Mansour. Wave propagation in the magnetic sun. *Center for Turbulence Research Proceedings of the Summer Program (IV. MAGNETOHYDRODYNAMICS)*, 2006.

[3] J. F. Ripoll, C. Jeffery, J. Zinn, and P. Colestock. Numerical investigations of lightning phenomena. *Center for Turbulence Research Proceedings of the Summer Program (IV. MAGNETOHYDRODYNAMICS)*, 2006.

[4] S. U. S. Choi. Enhancing thermal conductivity of fluids with nanoparticles. *ASME-Publications-Fed*, 231:99–106, 1995.

[5] V. Trisaksri and S. Wongwises. Critical review of heat transfer characteristics of nanofluids. *Renewable and Sustainable Energy Reviews*, 11.3:512–523, (2007).

[6] S. Özerinç, S. Kakaç and A. G. Yazıcıoğlu. Enhanced thermal conductivity of nanofluids: a state-of-the-art review. *Microfluidics and Nanofluidics*, 8.2:145–170, (2010).

[7] X. Q. Wang and A. S. Mujumdar. Heat transfer characteristics of nanofluids: a review. *International journal of thermal sciences*, 46.1:1–19, (2007).

[8] X. Q. Wang and A. S. Mujumdar. A review on nanofluids-part i: theoretical and numerical investigations. *Brazilian Journal of Chemical Engineering*, 25.4:613–630, (2008).

[9] Y. Li, J. Zhou, S. Tung, E. Schneider, and S. Xi. A review on development of nanofluid preparation and characterization. *Powder Technology*, 196.2:89–101, (2009).

[10] S. Kakaç and A. Pramuanjaroenkij. Review of convective heat transfer enhancement with nanofluids. *International Journal of Heat and Mass Transfer*, 52.13:3187–3196, (2009).

[11] K. Hiemenz. Die grenzschicht an einem in den gleichformingen flussigkeitsstrom eingetauchten graden kreiszylinder. *Dinglers Polytech. J.*, 326:321–324, 1911.

[12] J.T. Stuart. The viscous flow near a stagnation point when the external flow has uniform vorticity. *J. Aerospace Sci*, 26:124–125, 1959.

[13] F. Homman. Der einfluss grosser zahigkeit bei der stromung um den zylinder und um die kugel. *Z. Angew. Math. Mech.*, 16:153–164, 1936.

[14] L. Howarth. The boundary layer in three dimensional flow - part ii, the flow near a stagnation point. *Philosophical Magazine and Journal of Science Series 7*, 42.335:1433–1440, 1951.

[15] M. A. A. Hamad and M. Ferdows. Similarity solution of boundary layer stagnation-point flow towards a heated porous stretching sheet saturated with a nanofluid with heat absorption/generation and suction/blowing:a lie group anal-

ysis. *Communications in Nonlinear Science and Numerical Simulation*, 17.1:132–140, 2012.

[16] S. Nadeem, R. Mehmood, and N. S. Akbar. Non-orthogonal stagnation point flow of a nano non-newtonian fluid towards a stretching surface with heat transfer. *International Journal of Heat and Mass Transfer*, 57(2):679–689, 2013.

[17] S. Nadeem, A. Rehman, K. Vajravelu, J. Lee, and C. Lee. Axisymmetric stagnation flow of a micropolar nanofluid in a moving cylinder. *Mathematical Problems in Engineering*, 2012, 2012.

[18] S.Bhattacharyya and A. S. Gupta. Mhd flow and heat transfer at a general three-dimensional stagnation point. *International journal of non-linear mechanics*, 33.1:125–134, 1998.

[19] B. J. Gireesha, B. Mahanthesh, I. S. Shivakumara, and K. M. Eshwarappa. Melting heat transfer in boundary layer stagnation-point flow of nanofluid toward a stretching sheet with induced magnetic field. *Engineering Science and Technology, an International Journal*, 19(1):313–321, 2016.

[20] S. Nadeem, R. Mehmood, and N. S. Akbar. Combined effects of magnetic field and partial slip on obliquely striking rheological fluid over a stretching surface. *Journal of magnetism and magnetic materials*, 378:457–462, 2015.

[21] N. F. M. Noor, R. U. Haq, S. Nadeem, and I. Hashim. Mixed convection stagnation flow of a micropolar nanofluid along a vertically stretching surface with slip effects. *Meccanica*, 50(8):2007–2022, 2015.

[22] N. S. Akbar, S. Nadeem, R. U. Haq, and Z. H. Khan. Radiation effects on mhd stagnation point flow of nano fluid towards a stretching surface with convective boundary condition. *Chinese Journal of Aeronautics*, 26(6):1389–1397, 2013.

[23] R. U. Haq, S. Nadeem, Z. H. Khan, and N. S. Akbar. Thermal radiation and slip effects on mhd stagnation point flow of nanofluid over a stretching sheet. *Physica E: Low-dimensional Systems and Nanostructures*, 65:17–23, 2015.

[24] O. D. Makinde, W. A. Khan, and Z. H. Khan. Buoyancy effects on mhd stagnation point flow and heat transfer of a nanofluid past a convectively heated stretching/shrinking sheet. *International Journal of Heat and Mass Transfer*, 62:526–533, 2013.

[25] W. Ibrahim, B. Shankar, and M. M. Nandeppanavar. Mhd stagnation point flow and heat transfer due to nanofluid towards a stretching sheet. *International Journal of Heat and Mass Transfer*, 56(1):1–9, 2013.

[26] S. Mansur, A. Ishak, and I. Pop. The magnetohydrodynamic stagnation point flow of a nanofluid over a stretching/shrinking sheet with suction. *PLoS one*, 10(3):e0117733, 2015.

[27] T. Hayat, M. Imtiaz, A. Alsaedi, and M. A. Kutbi. Mhd three-dimensional flow of nanofluid with velocity slip and nonlinear thermal radiation. *Journal of Magnetism and Magnetic Materials*, 396:31–37, 2015.

[28] C. Zhang, L. Zheng, X. Zhang, and G. Chen. Mhd flow and radiation heat transfer of nanofluids in porous media with variable surface heat flux and chemical reaction. *Applied Mathematical Modelling*, 39(1):165–181, 2015.

[29] S. Dinarvand, A. Doosthoseini, E. Doosthoseini, and M. M. Rashidi. Series solutions for unsteady laminar mhd flow near forward stagnation point of an impulsively rotating and translating sphere in presence of buoyancy forces. *Nonlinear Analysis: Real World Applications*, 11(2):1159–1169, 2010.

[30] L. Howarth. Xxv. the boundary layer in three dimensional flow.part i. derivation of the equations for flow along a general curved surface. *The London, Edin-*

burgh, and Dublin Philosophical Magazine and Journal of Science, 42.326:239–243, 1951.

[31] A. Davey. Boundary-layer flow at a saddle point of attachment. *Journal of Fluid Mechanics*, 10.04:593–610, 1961.

[32] J. C. Maxwell Garnett. Colours in metal glasses and in metallic film. *Proceedings of the Royal Society of London*, 1904.

[33] H. C. Brinkman. The viscosity of concentrated suspensions and solutions. *The Journal of Chemical Physics*, 20(4):571–571, 1952.

[34] B. C. Pak and Y. I. Cho. Hydrodynamic and heat transfer study of dispersed fluids with submicron metallic oxide particles. *Experimental Heat Transfer an International Journal*, 11(2):151–170, 1998.

[35] Y. Xuan and W. Roetzel. Conceptions for heat transfer correlation of nanofluids. *International Journal of heat and Mass transfer*, 43(19):3701–3707, 2000.

[36] G. G. Stokes. *On the effect of the internal friction of fluids on the motion of pendulums*, volume 9. 1851.

[37] J. Vogel-Prandtl. Ludwig prandtl. 2014.

[38] L. Howarth. Cxliv. the boundary layer in three dimensional flow.part ii. the flow near a stagnation point. *The London, Edinburgh, and Dublin Philosophical Magazine and Journal of Science*, 42(335):1433–1440, 1951.

[39] H. F. Oztop and E. Abu-Nada. Numerical study of natural convection in partially heated rectangular enclosures filled with nanofluids. *International Journal of Heat and Fluid Flow*, 29(5):1326–1336, 2008.

[40] M. E. Yazdi, Alireza K. Nejad, S. Dinarvand, and H. Tamim. Brownian motion effects on natural convection of alumina–water nanofluid in 2-d enclosure. *Heat TransferAsian Research*, 43(8):720–733, 2014.

[41] S. Dinarvand, R. Hosseini, E. Damangir, and I. Pop. Series solutions for steady three-dimensional stagnation point flow of a nanofluid past a circular cylinder with sinusoidal radius variation. *Meccanica*, 48(3):643–652, 2013.